

Characterization of Pedot: Pss Functionalized by Dimethyl Sulfoxide and Triton X-100 and Tio₂ Nanoparticles

Anisa Yaseen^{1,2*}, A Vázquez-López², D Maestre², J Ramírez-Castellanos³, E S Marstein¹, S Z Karazhanov¹ and A Cremades²

¹Department for Solar Energy, Institute for Energy Technology, 2027 Kjeller, Oslo, Norway

²Department of Materials Physics, Faculty of CC. Physics, Complutense University of Madrid, Spain

³Department of Inorganic Chemistry, Faculty of CC Chemistry, Complutense University of Madrid, Spain

Abstract

In this work poly (3, 4-ethylenedioxythiophene)/poly(styrenesulfonate) (PEDOT:PSS) dispersed in solvent (5wt.% Dimethyl sulfoxide DMSO & 0.1wt.% Triton X-100) has been studied in pure form and when functionalized with TiO₂ nanoparticles. A preliminary characterization of bare PEDOT:PSS and romarchite TiO₂ nanoparticles synthesized by hydrolysis were firstly carried out. PEDOT:PSS was deposited on n(FZ)-Si by spin coating method. The influence of a piranha pre-treatment on the Si surface has been evaluated in this work, as well as the effects due to the presence of TiO₂ nanoparticles in the polymer. After achieving good adhesion and passivation of Si surface, the heterostructure has been characterized systematically by means of Raman spectroscopy using a He-Cd ($\lambda = 325$ nm) laser as excitation source, atomic force microscopy (AFM), scanning electron microscopy (SEM) and photoluminescence (PL) spectra, and PL image. Spatial homogeneity of the film composition on surface has been achieved. Uniform defect distribution and presence of charged defects, material quality and vibrational structure have been studied. PEDOT:PSS thin film was obtained through solution process which involves adding a solvent additive and/or conducting post treatment at low temperatures. The film was obtained by static spin coating method on a n-type silicon substrate, followed by annealing of the film at 120°C for 10-15 min. The achieved PEDOT:PSS layer thickness was around to be ~100 nm with the average surface roughness of 3.5±0.5 nm measured by AFM. Charge carrier lifetime measured by PL-machine was found out to be between 264-375 μ s. By four probe measurements, the sheet resistance was found out to be 338 Ω /sq

Keywords: Organic/Si interface • PEDOT:PSS • Si-surface passivation

Introduction

In recent years, organic polymers have attracted increased research interest in solar cells due to their light weight, low deposition cost at ambient conditions, solution based manufacturability, p-type electrical conductivity, excellent adhesion to other inorganic films. The organic-Si hybrid solar cells have already shown the capacity to further reduce the cost of the cells providing high efficiency at the same time. Within the last few years, reported efficiencies of the hybrid cells have increased very fast, with 12.3% [1] and 13% [2] in 2013, 17.1 % [3] in 2014, 18.3% on n-Si wafers and 20.6% on p-type Si wafers [4] as well as 13.3% efficiency 20 μ m thick Si cells [5] in 2015. If this trend can be continued, the ultimate efficiency expected for Si wafer-based cells ~30% [6] can be reached within a few years. Despite the efficiency progress within the very short time, there are unresolved challenges that are limiting production of the solar cells in commercial scale.

The performance of solar cells is not only determined by the quality of materials, but also by the interface between components of the device [7], which is characterized by the positions of energy levels of the Si and the organic compound, the band alignment and interface states that can act as recombination centers and trap charge carriers. It is therefore crucial for the project to control the interface and develop an efficient method to passivate the Si surface, without adding additional large costs. In commercial Si solar cells commonly inorganic compounds are used, such as SiNx, SiO₂, Al₂O₃, etc. all of which may provide low SRV values ~1 cm/s.

The deposition of such layers is however performed using expensive processing tools at relatively high temperatures and require special pre-treatments of Si surface. In contrast, polymers can be deposited at room temperature without special pre-treatments of Si surface [8] which is advantage of them compared to inorganic compounds. Whereas high efficiency Si-PEDOT:PSS solar cells have been developed successfully, there are very few studies of Si-PEDOT interface (see, e.g., Refs. [8-12]). In these high efficiency Si-PEDOT:PSS solar cells [3] an advanced passivation scheme using SiO₂ has been applied. In this study we synthesized PEDOT:PSS thin film on a n-Si substrate. Through solvent treatments of PEDOT:PSS-water mixed with an organic solvent such as DMSO and Triton x-100, carrier

lifetime is also enhanced. Adhesion to n-Si and surface morphology of PEDOT:PSS thin films, composition, presence of charge, carrier lifetime, recombination mechanisms, interface characterization have been discussed.

Method

Poly (3, 4-ethylenedioxythiophene): poly (4-styrenesulfonate)

The conducting polymer of poly (3, 4-ethylenedioxythiophene): poly (4-styrenesulfonate) (PEDOT:PSS) is one of the most important and regularly investigated organic conducting material. Through solvent treatment such as organic solvent with high boiling point, (Dimethyl sulfoxide (DMSO), ethylene glycol (EG)) and other methods such as spin coating, drop casting and diluting filtration one can enhance the conductivity.

Thin film synthesis

PEDOT:PSS (PH100 Clevios) with volume ratio of PEDOT to PSS (1:2.5) respectively was dispersed in solvent (5wt.% DMSO & 0.1wt.% Triton X-100). The n(FZ)-Si wafers with surface resistivity 1-5 Ω cm were used. PEDOT:PSS (PH100 Clevios) was modified by doping different weight percentages of DMSO up to 5% and Triton X-100 upto 0.1%. The solutions of the doped PEDOT:PSS were stirred for 2 hours at room temperature to obtain uniform dispersion. To remove traces of macroscopic aggregates, the precursor solutions were then filtered by using filters of pore size 0.45 μ m prior to preparation of thin films. Initially PEDOT:PSS dispersion were dropped onto a glass

Address for Correspondence: Anisa Yaseen, Department for Solar Energy, Institute for Energy Technology, 2027 Kjeller, Oslo, Norway, Tel (+47) 41112751; E-mail: anisa.yaseen@fys.uio.no

Citation: Anisa Yaseen, A Vázquez-López, D Maestre, J Ramírez-Castellanos, E S Marstein, S Z Karazhanov and A Cremades (2020) Characterization of Pedot: Pss Functionalized By Dimethyl Sulfoxide and Triton X-100 and Tio₂ Nanoparticles. *J Nanosci Curr Res* 5: 133.

Copyright: © 2020 Anisa Yaseen, et al. This is an open-access article distributed under the terms of the Creative Commons Attribution License, which permits unrestricted use, distribution, and reproduction in any medium, provided the original author and source are credited.

Received 17 November, 2020; **Accepted** 26 November, 2020; **Published** 03 December, 2020

substrate and n-Si substrate at different rpm for different times.

After each deposition the sheet resistance of PEDOT:PSS on glass substrate were measured and PL-imaging measurements of PEDOT:PSS on n(FZ)-Si substrate were made.

These initial steps were needed for deciding the deposition parameters. Both static and dynamic spin coating processes were used after running several test studies dynamic spin coating process was preferred. Dynamic spin coating is a process of depositing uid while the substrate is turning at low speed, usually of about 500 rpm. After depositions the sample is accelerated to a higher speed (typically in the range from 1500-6000 rpm) to thin out the material to achieve desired thickness. This type of process spread the liquid over the substrate without wasting a lot of material. The other reason for selecting this method is because with this process it is not necessary to deposit huge amount of material to wet the entire surface. This method is advantageous when the wettability of the material or substrate is poor. Once passivation was achieved and deposition parameters were decided then different techniques were used for analyzing the sample. The films were developed on n(FZ)-Si(100) substrate with resistivity 1-5 Ωcm , a diameter 9.80-10.20 mm and thickness $280.00 \pm 20.00 \mu\text{m}$. The PEDOT:PSS solutions were coated by employing dynamic coating method and by using the spin coating unit (Laurell, max speed 12000 rpm). The sample was spun and a small amount of solution was dropped on top of spinning n-Si substrate immediately. The spin coating process was carried out at two different rotation speeds, at 2000 rpms for 50 seconds and at 6000 rpms for 20 seconds, finally stopping until 0 rpms for 10 seconds. Two different rotations were needed for better surface passivation, since by employing one rotational speed the solution were either thrown away from the substrate, or the film were not smooth enough. Uneven film formation and aggregated were visible with naked eye. The prepared thin films on top of n(FZ)-Si were annealed at 120 °C for 10-15 min under ambient conditions to remove the moisture from the thin films. Thermal annealing is a critical step for removing access water and for acquiring good morphology, higher transparencies and higher conductivity of PEDOT:PSS films. By enhancing the conductivity of PEDOT:PSS thin films through annealing process the properties of PEDOT:PSS can also be improved. In this process it was found that the use of organic solvent with high boiling point can lead swelling and aggregation of PEDOT rich particles [13-18].

Characterization Methods

The sheet resistance of doped PEDOT:PSS measured in deposition over glass was $R_s = 330\text{-}338 \Omega/\text{sq}$. Electrical conductivity values were extracted from sheet resistance measurements carried out using a four-point probe resistivity measurement system. The electrical conductivity of PEDOT:PSS with 5% DMSO and 0.1% Triton X-100 was then found by using the formula:

$$\sigma = 1/(R \times l) = 1/\rho \cong 296.86 [S \times \text{cm}^{-1}]$$

where $R = 338 \Omega/\text{sq}$ is the measured sheet resistance, $l = 100 \text{ nm} = 1 \times 10^{-5} \text{ cm}$ is the thickness of the film.

The structural analysis of doped PEDOT:PSS thin films were carried out using scanning electron microscope (LEO-LEICA Stereoscan 440) and atomic force microscope (Nanotec electronica) to study the surface morphology of the prepared thin films. Raman and Photoluminescence spectrum were measured by using a red laser ($\lambda = 633 \text{ nm}$) and UV light ($\lambda = 325 \text{ nm}$) respectively in confocal microscope unit (Horiba Jobin-Yvon LabRam HR800), the acquired data was analyzed with LabSpac.5 software.

SEM imaging of PEDOT:PSS were carried out at room temperature

using SEM equipped with tungsten filament, Bruker nano Analyzer. The vacuum inside column gun was attained at a pressure value approximately 10-005 Torr, while the other important parameters such as the applied current and voltage was chosen to be $I_{\text{probe}} = 200 \text{ pA-1nA}$, and $\text{EHT} = 10\text{-}15 \text{ kV}$. At first the current and voltage was chosen to be 200 pA and 10 kV respectively in order to avoid damage, later on the current and voltage was increased to acquire better results without inducing much damage to the sample under examination. SEM images at various magnifications, EDS spectra and EDS maps were acquired and analyzed by using (Bruker Nano Analyticer) software. AFM imaging of PEDOT:PSS were carried out at room temperature using Nanotec electronica equipped with Dulcinea Control unit. The AFM was operated in the contact mode using 450 μm long V-shape silicon nitride cantilever, detector side coated with Al. The nominal force constant of the cantilever is 0.2N/m. The image data were collected in the detection mode with a loading force of typically 1nN and at a scan rate of typically 0-9 Hz. Statistical analysis of AFM micrographs was performed by using the WSxM-3.4 data processing software [18-23].

Results and Discussion

PL-Imaging

Hybrid n-Si/PEDOT:PSS was fabricated by following standard solution based process, PEDOT:PSS mixed with 5% DMSO and 0.1% Triton x-100 was spin coated at spin speed (500rpm - 6000rpm). This process resulted in achieving a polymer film thickness of 100 nm. The sheet resistivity of the film was measured by four point probe method, and was found out to be 338 Ω/sq . Initially we started with static dispense and only DMSO as a solvent which turn out to be poor choice of spin coating method, since the samples were getting scratched by manually spreading the liquid prior to turning on the machine. The other issue is that during the static spin coating large amount of liquid will be waste. Our sample required a larger puddle of liquid to ensure full coverage of the sample. In some cases the sample were not being coated properly and one could see an uneven coating with naked eye. This occurred due to the wettability and static spin coating dispense. In order to overcome this challenge, dynamic dispense was chosen and to achieve better wettability mixed co-solvent engineering of PEDOT:PSS were suggested [24-25], which has led to better passivation and conductivity. In order to check the passivation quality, the PL-images were taken by PL-machine and the carrier lifetime was measured which was increased from 170 μs to 280 μs . Figure 1 depicts the mean carrier lifetime of two samples with PEDOT:PSS deposited on n-Si substrate. Sample on the left (a) has been annealed longer for approximately 15 min whereas the other sample (b) was annealed for 10 min, annealing improved the charge carrier lifetime.

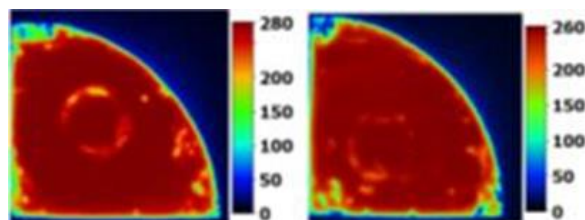


Figure 1: Photoluminescence images of PEDOT:PSS on n-Si wafer annealed for 10-15 min. The bars at the right side of each image represent the colour scale corresponding to average carrier lifetime [μs].

SEM Analysis

Figure 2 presents SEM images for the undoped and 0.5 wt% TiO_2 -doped PEDOT:PSS films. Analysis of the images shows smooth and

plain surface for different regions of the films. Surface of the films doped with 0.5% TiO₂, contains aggregates of nano-particles. Compositional analysis has been performed by EDX spectra and mapping [Figure 3-5]. In figure 4 the largest peak corresponds to the Si substrate, while the other smaller peaks are the elements such as sulfur, carbon, and oxygen. The peaks corresponding to Ti is shown up in the TiO₂ doped PEDOT:PSS. Peaks in energy range between 0.5-1.3 keV are from the well-known bremsstrahlung background noise.

Figure 5: Energy dispersive x-ray (EDX) mapping of PEDOT:PSS spin coated on n-Si substrate, the region can be seen in figure [2a] from where the EDX pattern was taken. Figure a) Green map represents Silicon, b) Turkish-blue represent Sulfur and c) pink and d) blue represent Carbon and Oxygen respectively.

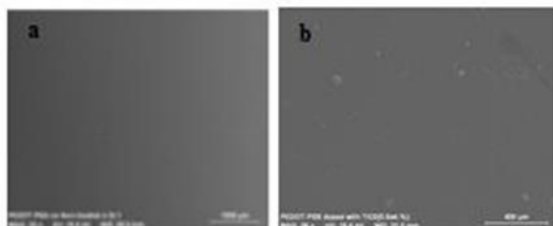


Figure 2: SEM Image of undoped PEDOT:PSS.

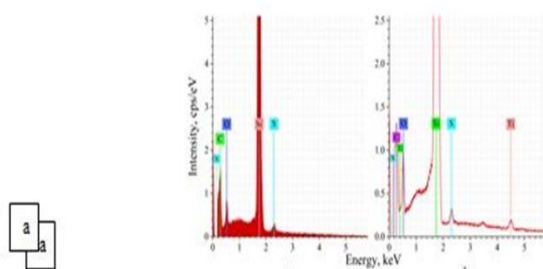


Figure 3: SEM Image of TiO₂ doped PEDOT:PSS. White patches shows TiO₂ nano particle aggregates/clusters.

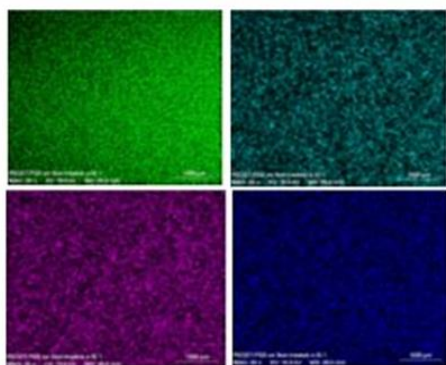


Figure 4: Energy dispersive x-ray (EDX) spectrum of (a) undoped and (b) TiO₂-doped PEDOT:PSS on n-Si substrate. The highest peak is of Si, while the other peaks represent Carbon, Oxygen, Sulfur and TiO₂.

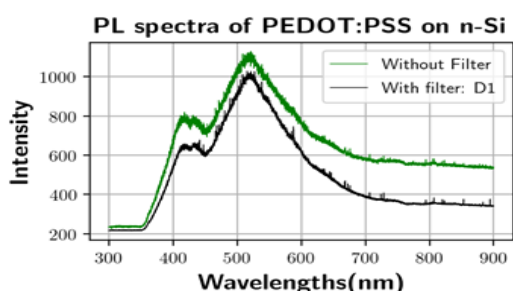


Figure 5: PL spectra of PEDOT:PSS deposit on n-Si substrate. Green plot represent the PL-spectra of PEDOT:PSS without using any filter, the signal is noisy, whereas black spectra was measured using natural filter, the noise is reduced slightly.

Photoluminescence Spectra

To get an insight into the charge extraction properties of the photo-generated carriers, the sample photoluminescence (PL) spectra were measured [Figure 6 and 7] at room temperature. Two emission peaks were detected at wavelengths 415 nm and 520 nm. The emission peak centered at 520 nm spans a wavelength range from 450 nm to 600 nm, while the second peak centered at 415 nm spans a wavelength range from 400 nm to 450 nm. Comparing with other studies it is confirmed that the PL is emitted from PSS at 400 nm, the peaks observed at 415nm is c=c stretching, coincide well with other studies [26-27].

Figure 7 presents degradation analysis based on PL-spectra measured from the same spot twice. The sample was irradiated with UV light during ~2 minutes. The red and black color lines show the PL-spectra acquired 1st and 2nd time respectively. The PL intensity has clearly been reduced considerably, which indicates the degradation of the PEDOT:PSS, fortunately upon using natural filter degradation can be avoided (Figure 8).

We found that the PEDOT:PSS film gets destroyed by the irradiation [Figure 9 on the right], where the blue curve represents the Raman spectra of PEDOT:PSS and magenta curve represents the spectra of a damaged region (the region where spectra was retaken from). All the other PEDOT and PSS peaks are completely disappeared expect one (PEDOT) at 1417.43 cm⁻¹ and PSS at 982.86 cm⁻¹, but they have been reduced at considerable amount. Since the solution was doped with DMSO and Triton X-100, from the literature it is concluded that these solvents have a strong interaction both with PSS-chains and PEDOT-chain, which results in phase separation of PEDOT:PSS, thus promoting the ordered alignment of PEDOT [4]. From the Raman spectra of TiO₂-doped PEDOT:PSS, the sample can be clearly identified. Figure [8] shows the active modes of TiO₂, the distinct peak at Raman frequencies are (150cm⁻¹), (420cm⁻¹) and (630cm⁻¹). In crystalline structures only phonons close to the center of the Brillouin zone give rise to inelastic scatterings of incident beam. When the size of the crystal ranges in nano-meter scale, larger size of Brillouin zone contribute to the scattering process, which results in various Raman frequency peaks, thus one can observe the shape of Raman band. The mean peak of TiO₂ can be observed at 150(cm⁻¹).

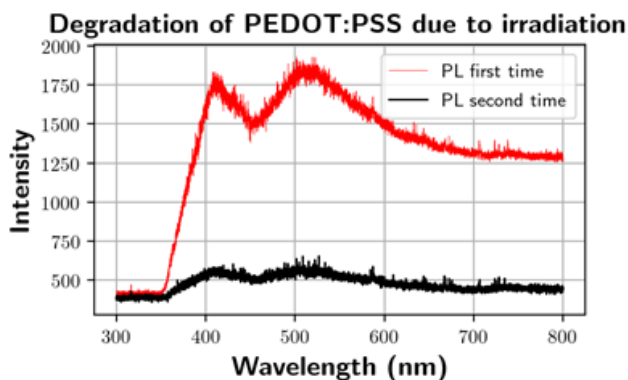


Figure 6: PL spectra of PEDOT:PSS on n-Si taken at same spot, red curve shows the PL measured at first, while the black curve shows PL measured second time at same the spot using UV light (λ = 325nm, with filter D=1). Irradiation time for each measurement was 2 i.e. total irradiation time was 4 min.

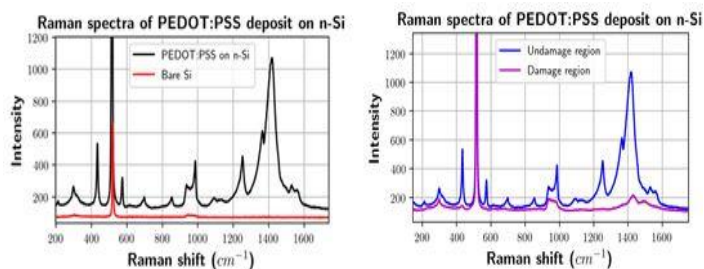


Figure 7: Raman spectra of PEDOT:PSS deposit on n-Si substrate. The spectra (black and red curves) on the top panel shows the comparison between Raman spectra of PEDOT:PSS on n-Si and Bare Si, while the spectra (blue and magenta) on the bottom panel shows the Raman spectra of an undamaged and damaged PEDOT:PSS on n-Si.

Raman spectra of PEDOT:PSS doped with TiO_2

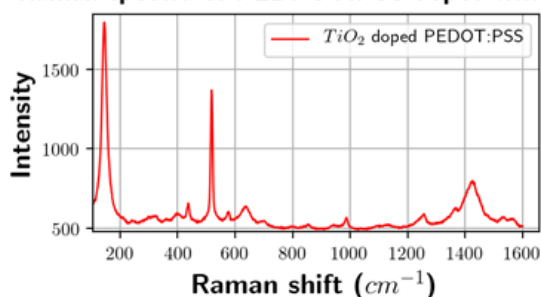


Figure 8: Raman spectra of PEDOT:PSS doped with 0.5 wt.% TiO_2 on n-Si substrate. The peak at around 450 cm^{-1} is distinct peak from TiO_2 , other smaller peaks at approximately 430 and 670 cm^{-1} are also originate from TiO_2 . The other peaks represents Si and PEDOT:PSS.

Atomic Force Microscopy

AFM Analysis

The AFM micrographs, reported in Figure [9], show some round-shaped bright domains randomly distributed on the film surface. These large granular domains have been associated by several reports with high-conducting PEDOT clusters with an enhanced size promoted by solvent annealing. In other words the PEDOT-rich and PSS-rich domains or aggregates can be due to the heat treatment in the annealing process. As we heat sample (with PEDOT:PSS deposit on top) at temperature 120°C , the PEDOT move to the film surface and get accumulated, giving rise to vertical phase separation and forming large grains [3]. On this basis, the grain-like structure that emerged for thicker films could be seen as a fingerprint of a thickness-dependent phase segregation process. We made a statistical analysis of the surface topographies shown in Figure [9]. This was done by evaluating the root mean square roughness RMS, a parameter expressing the measure of the topographical statistical fluctuations around an average surface height. Due to its length-scale invariant character, RMS can mirror the bulky redistribution of the two phases of diphasic polymeric blends and compounds upon thermally induced phase segregation and the related small grains coalescence. The topographic image 9 indicate that the films are quit homogeneous with RMS roughness of $(3.5 \pm 0.5 \text{ nm})$. The morphology of PEDOT:PSS consists of PEDOT:PSS grain like cluster/particles and of the excess of PSS located at the grain boundaries and the film surface, and thereby creating a polymer matrix [28-30].

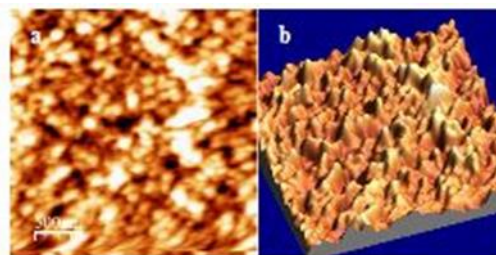


Figure 9: (a) AFM micro-graphs of PEDOT:PSS thin film. The scan area size is $2.5\mu\text{m}^2$, parabola filter was applied to enhance the appearance of different regions bright and dark regions on the right panel correspond to PEDOT-rich and PSS-rich grains respectively. (b) shows the corresponding 3D image of micrograph.

Conclusion

In this work hybrid composites formed by a conductive polymer PEDOT:PSS functionalized with TiO_2 nanoparticles have been investigated. The composites formed by PEDOT:PSS and TiO_2 nanoparticles (0.5 wt. %) were deposited on n-Si or glass substrates by spin-coating, leading to layers with a thickness around 120 nm and an average surface roughness of $3.5 \pm 0.5 \text{ nm}$, as measured by atomic force microscopy (AFM). In the spin coated films, the outer layer of the cluster is PSS-rich and the core of the cluster it PEDOT-rich. When the film is formed the PSS acts as a barrier to the conduction of the carries, the conduction is performed within the grains with hops from PEDOT-grains to another according to the hopping model. We show that co-solvent treatment rearranges the PEDOT, and removes the excess PSS from the surface which leads to charge transport in the film and thus increases the electrical conductivity. It has been observed that the surface of the films is quite homogeneous. The results indicate to possibility of further enhancement of the Si surface passivation by co-solvent engineering by increasing concentration of EG or using MeOH (methanol) as co-solvent with DMSO. PL-spectrum is found to be enhanced with increasing the thickness of the PEDOT:PSS film. Electrical and photoluminescence measurements were also performed in these samples. The influence of a piranha pre-treatment on the Si surface has been evaluated in this work, as well as the effects due to the presence of TiO_2 nanoparticles in the polymer. By Raman measurements, variations in the region $1200 - 1500 \text{ cm}^{-1}$ characteristic from the PEDOT:PSS were observed after continuous irradiation. Finally, the composites including TiO_2 nanoparticles were used for n-Si surface passivation. Lifetime values around $375 \mu\text{s}$ were measured by PL-QSSPC, which confirms good passivation behaviour of the film even without pre-treatment of the Si substrate.

Acknowledgements

This work was supported by the Spanish Ministry of Innovation, Science and Technology and Spanish Ministry of Economy through Research Projects MAT-2015-65274-R/FEDER, RTI2018-097195-B-I00 and M-ERA.NET PCIN-2017-106. SZK and ESM have received financial support from M-ERA.net project 272806 by the Research Council of Norway.

References

1. Wu S, Cui W, Aghdassi N, Song T, Duhm S, Lee ST, et al. Junction Adhesion: Nanostructured Si/Organic Heterojunction Solar Cells with High Open-Circuit Voltage via Improving Junction Quality. *Adv. Funct. Mater.* 26 (2016): 5035-41.

2. Wang Y, Shao P, Chen Q, Li Y, Li J, et al. Dependence of high density nitrogen-vacancy center ensemble coherence on electron irradiation doses and annealing time. *J Phys D Appl Phys.* 50 (2017).
3. Zhang X, Zhang B, Ouyang X, Chen L, Wu H. Polymer Solar Cells Employing Water-Soluble Polypyrrole Nanoparticles as Dopants of PEDOT:PSS with Enhanced Efficiency and Stability. *J Phys Chem C.* 121 (2017): 18378–84.
4. Zielke D, Niehaves C, Lövenich W, Elschner A, Hörteis M, Schmidt. Organic-silicon Solar Cells Exceeding 20% Efficiency. *J Energy Procedia.* 77 (2015): 331–9.
5. García-Tecedor M, Karazhanov SZ, Vásquez GC, Haug H, Maestre D, et al. Silicon surface passivation by PEDOT: PSS functionalized by SnO₂ and TiO₂ nanoparticles. *Nanotechnology.* 29 (2018).
6. Jäckle S, Mattiza M, Liebhaber M, Brönstrup G, Rommel M, et al. Junction formation and current transport mechanisms in hybrid n-Si/PEDOT:PSS solar cells. *Sci Rep* 5 (2015): 1-12.
7. Yameen M, Srivastava SK, Singh P, Turan K, Prathap P, et al. Nanostructured Black Silicon for Efficient Thin Silicon Solar Cells: Potential and Challenges. *J Mater Sci.* 50 (2015): 8046–56.
8. Pietsch M, Jäckle S, Christiansen S. Interface investigation of planar hybrid n-Si/PEDOT:PSS solar cells with open circuit voltages up to 645 mV and efficiencies of 12.6 %. *Appl Phys A Mater Sci Process.* 115 (2014): 1109-13.
9. Li L, Ma B, Xie H, Yue M, Cong R, Gao W, et al. Photocatalytic H₂ evolution for α -, β -, γ -Ga₂O₃ and suppression of hydrolysis of γ -Ga₂O₃ by adjusting pH, adding a sacrificial agent or loading a cocatalyst. *RSC Adv.* 6 (2016): 59450-6.
10. Delgado MR, Morterra C, Cerrato G, Magnacca G, Otero Areán C. Surface Characterization of γ -Ga₂O₃ : A Microcalorimetric and IR Spectroscopic Study of CO Adsorption. *Langmuir.* 18 (2002): 10255–60.
11. Chen T, Tang K. TiO₂ based metal-semiconductor-metal ultraviolet photodetectors *Appl Phys Lett.* 90 (2007): 3-6.
12. Hou Y, Wu L, Wang X, Ding Z, Li Z, Fu X. Photocatalytic performance of α -, β -, and γ -Ga₂O₃ for the destruction of volatile aromatic pollutants in air. *J Catal.* 250 (2007): 12–8.
13. Kang SM, Kang BK, Song YH, Yoon DH. Synthesis and structural properties of β -Ga₂O₃ nanoparticles by liquid phase precursor method. *Mater Sci Eng B Solid-State Mater Adv Technol.* 173 (2010): 105–8.
14. Shimamura K, Villora EG, Ujiie T, Aoki K. Electrical conductivity and carrier concentration control in β -Ga₂O₃ by Si doping. *Appl Phys Lett* 92 (2008): 2008-10.
15. Nærland TU, Angelskår H, Kirkengen M, Sondenå R, Marstein ES. The role of excess minority carriers in light induced degradation examined by photoluminescence imaging. *J Appl Phys* 112 (2012).
16. Trupke T, Bardos RA, Abbott MD, Chen FW, Cotter JE, et al. *Conf Rec 2006 IEEE 4th World Conf Photovolt Energy Conversion, WCPEC-4.* 1 (2007): 928–31.
17. Trupke T, Bardos RA, Abbott MD. Spatially resolved series resistance of silicon solar cells obtained from luminescence imaging. *Appl Phys Lett.* 87 (2005): 1–3.
18. López I, Lorenz K, Nogales E, Méndez B, Piqueras J, et al. Study of the relationship between crystal structure and luminescence in rare-earth-implanted Ga₂O₃ nanowires during annealing treatments. *J Mater Sci.* 49 (2014): 1279–85.
19. Schmidt J, Titova V, Zielke D. Organic-silicon heterojunction solar cells: Open-circuit voltage potential and stability. *Appl Phys Lett.* 103 (2013).
20. Yu P, Tsai C-Y, Chang J-K, et al. 13% efficiency hybrid organic/silicon-nanowire heterojunction solar cell via interface engineering. *ACS Nano.* 12 (2013): 10780-10787.
21. Zielke D, Pazidis A, Werner F, Schmidt J. Organic-silicon heterojunction solar cells on n-type silicon wafers: The BackPEDOT concept. *Solar Energy Materials and Solar Cells.* 131 (2014): 110-116.
22. Zielke D, Niehaves C, Lövenich W, et al. Organic-silicon Solar Cells Exceeding 20% Efficiency. *Energy Proc.* 77 (2015): 331-339.
23. He J, Gao P, Liao M, et al. Realization of 13.6% Efficiency on 20 μ m Thick Si/Organic Hybrid Heterojunction Solar Cells via Advanced Nanotexturing and Surface Recombination Suppression. *ACS Nano.* 9 (2015):6522-6531.
24. Saga T. Advances in crystalline silicon solar cell technology for industrial mass production. *NPG Asia Mater.* 2 (2010): 96-102.
25. Cao Y, Stavrinadis A, Lasanta T, et al. The role of surface passivation for efficient and photostable PbS quantum dot solar cells. *Nature Energy.* 1 (2016): 16035.
26. Biro D, Warta W. Low temperature passivation of silicon surfaces by polymer films. *Solar Energy Mater Solar Cells.* 71 (2002):369-374.
27. Li Y, Fu P, Li R, et al. Ultrathin flexible planar crystalline-silicon/polymer hybrid solar cell with 5.68% efficiency by effective passivation. *Appl Surf Sci.* 366 (2016): 494-498.
28. Zhang F, Liu D, Zhang Y, et al. Methyl/Allyl Monolayer on Silicon: Efficient Surface Passivation for Silicon-Conjugated Polymer Hybrid Solar Cell. *ACS Appl Mater Interfaces.* 11 (2013): 4678-4684.
29. Thomas JP, Zhao L, McGillivray D, Leung KT. High-efficiency hybrid solar cells by nanostructural modification in PEDOT:PSS with co-solvent addition. *J Mater Chem A.* 7 (2014): 2383-2389.
30. Thomas JP, Leung KT. Defect-Minimized PEDOT:PSS/Planar-Si Solar Cell with Very High Efficiency. *Adv Funct Mater.* 24 (2014): 4978-4985.